Journal of Photochemistry and Photobiology A: Chemistry 217 (2011) 100–107

Contents lists available at ScienceDirect

Journal of Photochemistry and Photobiology A: Chemistry

journal homepage: www.elsevier.com/locate/jphotochem

Effect of intraligand π-delocalization on the photophysical properties of two new Ru(II) complexes

Daniel A. Lutterman[a], Laurie A. Lazinski-Melanson[a], Yogen Asher[a], Dean H. Johnston[b], Judith C. Gallucci[a], Claudia Turro[a,*]

[a] Department of Chemistry, The Ohio State University, Columbus, OH 43210, United States
[b] Department of Chemistry, Otterbein College, Westerville, OH 43081, United States

ARTICLE INFO

Article history:
Received 20 August 2010
Received in revised form
23 September 2010
Accepted 27 September 2010
Available online 14 October 2010

Keywords:
Ruthenium complex
Excited state
Emission
Transient absorption

ABSTRACT

Two new Ru(II) complexes, $[Ru(bpy)_2(1\text{-}COO\text{-}iqu)]^+$ (**2**; bpy = 2,2′-bipyridine, 1-COO-iqu$^-$ = isoquinoline-1-carboxylate) and $[Ru(bpy)_2(3\text{-}COO\text{-}iqu)]^+$ (**3**; 3-COO-iqu$^-$ = isoquinoline-3-carboxylate), were prepared and their crystal structures solved. The ground and excited state properties of **2** and **3** were characterized and compared to those of $[Ru(bpy)_3]^{2+}$ (**1**). The presence of the oxygen atom in the Ru(II) coordination sphere makes **2** and **3** easier to oxidize than **1**. The Ru → bpy MLCT absorption and emission of **2** and **3** are red-shifted relative to that of **1** in CH_2Cl_2, and the E_{00} energies were estimated to be 1.89 eV and 1.95 eV from the low temperature emission of **2** and **3**, resulting in excited state oxidation potentials of −1.03 V and −1.10 V vs SCE, respectively. In addition to the short-lived emissive ^{3}MLCT state, a long-lived species is observed in the transient absorption of **3** in DMSO (τ = 49 μs) and pyridine (τ = 44 μs), assigned to a solvent-coordinated complex. This intermediate is not observed for **3** in non-polar solvents or for **2**. The absence of the solvent coordinated intermediate in **2** is explained by the stronger Ru–O bond afforded by the lower conjugation in that extends onto the carboxylic acid in the 1-COO-iquo$^-$ligand, compared to that in the 3-COO-iqu$^-$ligand in **3**. Transient absorption experiments also show that the ^{3}MLCT excited state of **3** is able to reduce methyl viologen.

1. Introduction

Emissive Ru(II) complexes have proved useful as the light-absorbing units in cells for solar energy conversion [1–4], biological sensing [5–11], and as therapeutics [12–14]. Owing to the requirement of strong luminescence or long-lived excited states for many of these applications, the investigation of the molecular features that affect the excited state properties of these complexes have focused on those that result in an increase in the emission intensity and lifetime [15–20]. Other photochemical applications of Ru(II) complexes, however, require greater yield of alternative photochemical products that often compete with luminescence, such as isomerization for photoswitching [21], high quantum yield photoaquation for DNA binding [22], photogenerated nitric oxide [23–25], and access of the ligand field states for applications of the complexes as molecular machines [15a,26].

It is well known that the emission from these systems, such as the prototypical complex $[Ru(bpy)_3]^{2+}$ (**1**; bpy = 2,2′-bipyridine) depends on the energy of the luminescent ^{3}MLCT state relative to the ground state and to the low-lying non-emissive ligand-field (^{3}LF) states [27]. In general, ligand exchange photochemistry takes place through the access of the ^{3}LF states, which posses Ru–L(σ*) character, such that their population results in ligand dissociation [27–30]. Photoinduced ligand exchange is common for Ru(II) complexes with monodentate ligands [31,32], however, such photochemistry stemming from bidentate ligands is not as efficient due to the chelate effect [28,32,33]. The photostability of complexes with bidentate ligands makes these systems useful for applications where chemical bonds must remain intact, such as in luminescent sensors.

In contrast, photoinduced switching applications require that a photochemical reaction take place, but this reactivity must be reversible. The 1,2-dithienylethene derivatives are examples of such a system, where switching between the ring open and ring closed isomers depends on the energy of light irradiation, such that one can be converted into the other upon photon absorption of a given wavelength [34,35]. Bistability is also exemplified in Ru(II) complexes with dimethyl sulfoxide (DMSO) ligands, where DMSO is able to coordinate to the ruthenium atom through either the sulfur (S-bound) or oxygen atom (O-bound) with the former being more thermodynamically stable [36]. The S-bound isomer is able to undergo isomerization to the O-bound complex by accessing the ^{3}MLCT excited state through irradiation with visible light [36].

* Corresponding author at: Department of Chemistry, The Ohio State University, 100 W. 18th Ave., Columbus, OH 43210, United States. Tel.: +1 6142926708.
E-mail addresses: turro.1@osu.edu, turro@chemistry.ohio-state.edu (C. Turro).

1010-6030/$ – see front matter © 2010 Elsevier B.V. All rights reserved.
doi:10.1016/j.jphotochem.2010.09.025

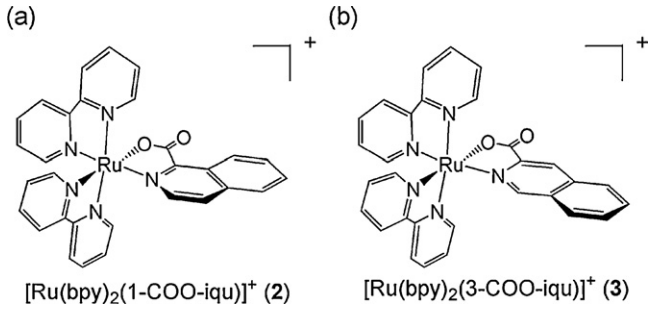

Fig. 1. Molecular structures of (a) **2** and (b) **3**.

In the present work, two new Ru(II) complexes are reported, $[Ru(bpy)_2(1\text{-}COO\text{-}iqu)]^+$ (**2**) and $[Ru(bpy)_2(3\text{-}COO\text{-}iqu)]^+$ (**3**) (1-COO-iqu$^-$ = isoquinoline-1-carboxylate, 3-COO-iqu$^-$ = isoquinoline-3-carboxylate), with molecular structures schematically depicted in Fig. 1. The 1-COO-iqu$^-$ and 3-COO-iqu$^-$ ligands coordinate to the Ru(II) center via an aromatic nitrogen and a carboxylate oxygen atom, which results in photophysical and redox properties different from those of $[Ru(bpy)_3]^{2+}$ (**1**). Steady-state and time-resolved emission, along with transient absorption experiments were used to characterize the processes that follow absorption of a photon by **2** and **3**. A long-lived intermediate is detected for **3** in coordinating solvents that is not observed in **2**. Calculations provide a basis to explain the differences observed for the two complexes under similar experimental conditions.

2. Experimental

2.1. General

Ruthenium chloride hydrate, 2,2′-bipyridine (bpy), isoquinoline-1-carboxylic acid (1-COOH-iqu), isoquinoline-3-carboxylic acid (3-COOH-iqu), and methyl viologen dichloride were purchased from Aldrich and used as received. $Ru(bpy)_2Cl_2$ was prepared by a published method and the product was subjected to numerous CH_2Cl_2/H_2O extraction cycles in order to remove any trace $[Ru(bpy)_3]^{2+}$ [37,38]. $[Ru(bpy)_3]^{2+}$ (**1**) was synthesized by typical methods and was precipitated from acetone/ether to remove remaining free ligand [39].

2.2. Synthesis

2.2.1. $[Ru(bpy)_2(1\text{-}COO\text{-}iqu)]^+$ (**2**)

$Ru(bpy)_2Cl_2$ (8 mg, 16.5 μmol) was stirred in 40 mL CH_2Cl_2/ethanol (80:20, v:v) with 1.2 equiv. of 1-COOH-iqu ligand overnight. The initially purple solution turned red, was dried, and the product was precipitated from acetone/ether. Further separation of free 1-COO-iqu$^-$ ligand and another unidentified product was accomplished by dissolving the mixture in ~20 mL of H_2O and elution through a Sephadex G-15 column with 50 mM NaCl. Two colored bands were apparent, and the second to elute, which was also the major product, was collected. The eluent was dried and the pure product was dissolved in CH_2Cl_2 and filtered to remove the solid NaCl. X-ray quality crystals of **2** were grown from layered CH_2Cl_2/n-heptane and the resulting structure is shown in Fig. 2a. The MS parent ion peak was observed at m/z = 586.1 for $[Ru(bpy)_2(1\text{-}COO\text{-}iqu)]^+$ with the expected isotope pattern corresponding to the ruthenium. ^{1}H NMR (400 MHz) in DMSO-d_6 (splitting, integration): 7.41 (m, 3H), 7.58 (m, 2H), 7.76 (t, 1H), 7.84 (m, 3H), 7.91 (d, 1H), 7.94 (d, 1H), 8.03 (m, 3H), 8.16 (m, 2H), 8.71 (d, 1H), 8.82 (m, 4H), 9.90 (d, 1H). Anal. Calcd. for $RuN_5O_2C_{30}H_{22}Cl–6H_2O$: C, 49.42; N, 9.60; H, 4.70. Found: C, 48.90; N, 9.00; H, 4.64.

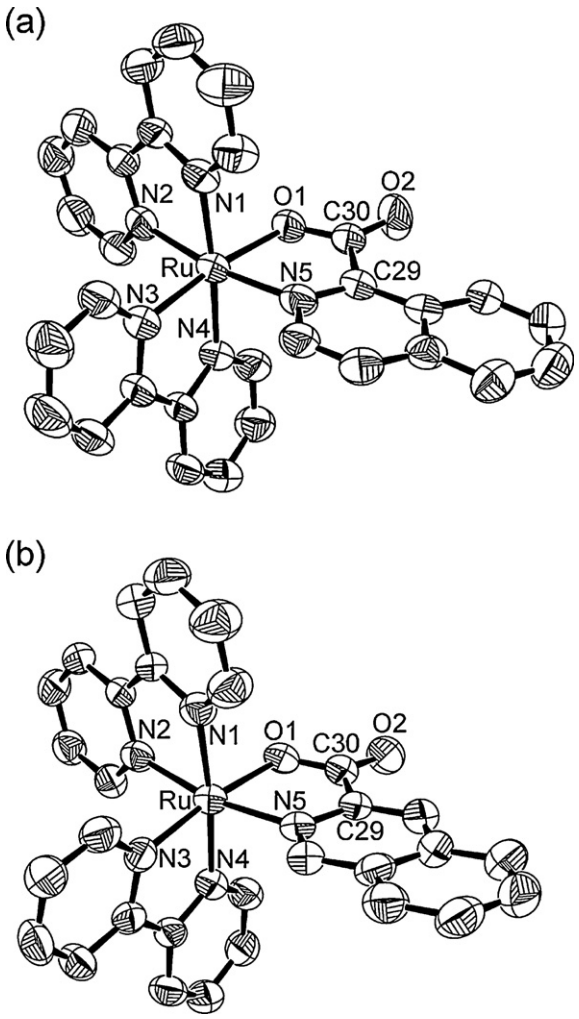

Fig. 2. ORTEP representation of (a) **2** and (b) **3** with thermal ellipsoids drawn at the 50% probability level. Hydrogen atoms were removed for clarity.

2.2.2. $[Ru(bpy)_2(3\text{-}COO\text{-}iqu)]^+$ (**3**)

The reaction of $Ru(bpy)_2Cl_2$ with 3-COOH-iqu and subsequent purification and crystal growth was accomplished by a method analogous to that described for **2**. The crystal structure of **3** is shown in Fig. 2b. The MS parent ion peak was observed at m/z = 586.1 for $[Ru(bpy)_2(3\text{-}COO\text{-}iqu)]^+$ with the expected isotope pattern corresponding to the ruthenium. ^{1}H NMR (400 MHz) in DMSO-d_6 (splitting, integration): 7.41 (m, 2H), 7.56 (t, 1H), 7.62 (d, 1H), 7.75 (m, 2H), 7.87 (m, 2H), 8.02 (m, 4H), 8.15 (m, 2H), 8.22 (d, 1H), 8.31 (s, 1H), 8.53 (s, 1H), 8.80 (m, 5H). Anal. Calcd. for $RuN_5O_2C_{30}H_{22}Cl–7H_2O$: C, 48.23; N, 9.37; H, 4.86. Found: C, 47.80; N, 8.70; H, 4.80.

2.3. Instrumentation and methods

Absorption measurements were performed on a Hewlett–Packard diode array spectrometer (HP8453) with HP8453 Win System software and emission spectra were collected on a SPEX FluoroMax-2 spectrometer. ^{1}H NMR spectra were recorded on a Bruker DRX-400 spectrometer. The identities of **2** and **3** in solution were confirmed by electrospray mass spectrometry (Micromass Q-Tof II, Waters) and carbon, nitrogen, and hydrogen elemental analysis (Galbraith Laboratories, TN). Cyclic voltammetry measurements were performed in CH_3CN with 0.1 M Bu_4NPF_6 as the supporting electrolyte on a BAS CV-50W (Version 2.3) instrument with a single-compartment three-electrode cell.

The working electrode was a 1.0-mm diameter Pt disk (BAS) with a Pt wire auxiliary electrode and a Ag/Ag^+ pseudo-reference electrode. Ferrocene (Fc) was used as a reference under the same experimental conditions with $E_{1/2}(Fc^{+/0}) = +0.43$ V vs SCE [40].

Deoxygenation for the luminescence experiments was performed by bubbling the sample with argon for ~15 min and keeping it under positive argon pressure during the experiment. Emission quantum yields (Φ_{em}) were calculated using $[Ru(bpy)_3]^{2+}$ in CH_2Cl_2 ($\Phi_{em} = 2.9 \times 10^{-2}$) as the reference actinometer by well-established methods [41,42]. The emission lifetimes and transient absorption signal were measured following sample excitation with the 532 nm output from a frequency doubled Spectra-Physics GCR-150-10 Nd:YAG laser (fwhm ~8 ns, ~5 mJ/pulse) with a home built system previously described in detail [43]. Attenuated scattered laser light yielded an overall instrument response function with fwhm = 12.5 ns. Emission lifetime measurements in DMSO were collected using a time-correlated single photon counting instrument previously described pumped by a Nd-YLF laser (Coherent Antares 76-s) used to pump a dye laser (Coherent 700 series, stilbene, tunable 410–480 nm, 1–4 MHz) with $\lambda_{exc} = 470$ nm (fwhm ~3 ps) and with a ~40 ps instrument response [44].

Both crystals of **2** and **3** were very thin, fragile red plates. Data collections were done on a Nonius Kappa CCD diffractometer at 200 K using an Oxford Cryosystems Cryostream Cooler. The data collection strategy was designed to measure a quadrant of reciprocal space with a redundancy factor of 4 for both $[Ru(bpy)_2$(1-COO-iqu)]Cl and $[Ru(bpy)_2$(3-COO-iqu)]Cl, such that 90% of the reflections in each quadrant were measured at least 4 times. A combination of phi and omega scans with a frame width of 1.0° was used. For **3**, data was collected only out to a maximum 2θ value of 45° because of the weakness of the diffraction pattern. Data integration was performed with Denzo [45], and scaling and merging of the data was performed with Scalepack [45]. Crystallographic details for both complexes are summarized in Table S1.

Both $[Ru(bpy)_2$(1-COO-iqu)]Cl and $[Ru(bpy)_2$(3-COO-iqu)]Cl were determined to be $P2_1/n$ by the teXsan package [46] based on systematic absences and the intensity statistics. The structures were solved by the Patterson method in SHELXS-86 [47]. Full-matrix least-squares refinements based on F^2 were performed in SHELXL–97 [48]. In both **2** and **3** the asymmetric unit contains the Ru complex, a chloride ion and a region of disordered solvent. It was difficult to model this disordered region and to even identify which peak in the electron density map was the Cl^- ion for both structures. In order to solve this problem for **2**, one of the top peaks in the difference map, which was not near any of the other peaks, was assigned as the Cl^- ion. No atoms were assigned in the rest of this disordered region, and the SQUEEZE [49] program of PLATON [50] was used to handle the solvent problem. This disordered region occupies 911 $Å^3$ per unit cell, and the electron density removed by SQUEEZE is 258 electrons per unit cell.

Similarly, in $[Ru(bpy)_2$(3-COO-iqu)]Cl, the asymmetric unit contains a disordered region of chloride ions and/or CH_2Cl_2 molecules. There are five obvious peaks in the disordered region and none are within bonding range of each other. The five peaks were refined as chlorides with their occupancy factors refined independently. For both structures, the hydrogen atoms were included in the model at calculated positions using a riding model with $U(H) = 1.2 * Ueq$ (attached atom). Neutral atom scattering factors were used and included terms for anomalous dispersion [51].

The gas-phase molecular and electronic structure determinations on complexes **1**–**3** and the 1-COO-iqu$^-$ and 3-COO-iqu$^-$ free ligands were performed with density functional theory (DFT) using the Gaussian03 program package [52]. The B3LYP [53–55] functional together with the 6-31G* basis set was used for H, C, N, and O [56], along with the Stuttgart/Dresden (SDD) energy-consistent pseudopotentials for Ru [57,58]. All geometry optimizations were performed in C_1 symmetry with subsequent frequency analysis to show that the structures are local minima on the potential energy surface. Solvent effects were modeled by single point calculations based on the gas-phase optimized structures using the polarizable continuum model (PCM) [59,60]. Molecular orbitals were visualized using Molekel 4.3.win32 [61]. The vertical singlet transition energies of the complexes were computed at the time-dependent density functional theory (TD-DFT) level by using the gas-phase optimized structure for the ground state. The relative energies of the free ligands, 1-COO-iqu$^-$ and 3-COO-iqu$^-$, were computed as the carboxylate substituent was rotated relative to the isoquinoline unit. First, the ground state for each of the free ligands was determined with the same functional and basis set used for **2** and **3** and confirmation that the computed structures were local minima on the potential energy surface was accomplished by a frequency analysis. Then, the dihedral angle θ(N5–C29–C30–O1), was adjusted such that the carboxylate group was rotated in increments of 10° relative to the isoquinoline unit and single point energy calculations were computed.

3. Results and discussion

3.1. Synthesis and characterization

Complexes **2** and **3** were synthesized from the reaction of purified $Ru(bpy)_2Cl_2$ (bpy = 2,2′-bipyridine) with a slight excess of the corresponding isoquinoline carboxylic acid in CH_2Cl_2/ethanol. The crystal structures of **2** and **3** are shown in Fig. 2, and data collection parameters listed in Supporting Information (Table S1). The bidentate coordination of the isoquinoline carboxylate ligands through the aromatic nitrogen and one of the carboxylate oxygen atoms affords a pseudo-octahedral environment around the Ru(II) metal center, with selected bond distances shown in Fig. 3a. All Ru–N bonds from the nitrogen atoms in the bpy or isoquinoline ligands in **2** and **3** are of similar length, ranging from 2.026(6) Å to 2.052(5) Å, and parallel the corresponding bond distances reported for $[Ru(bpy)_3]^{2+}$, which average 2.057(3) Å [62,63]. Structural differences surrounding the coordinated isoquinoline carboxylate ligand are observed in **2** and **3**, showing a longer C(29)–C(30) bond length in **2**, 1.531(8) Å, relative to that in **3**, 1.481(12) Å (Fig. 3a). Gas phase molecular structure calculations also predict a slightly longer C(29)–C(30) bond length in **2** (1.536 Å) relative to that of **3** (1.518 Å). The lengthening of this bond in **2** compared with **3** is indicative of reduced conjugation between the isoquinoline ring and the carboxylate moiety in the former, resulting in greater negative charge on the oxygen atom coordinated to the metal center, O(1). As such, the Ru–O(1) bond length is shorter in **2** than in **3**, 2.061(4) Å and 2.088(5) Å, respectively (Fig. 3a), indicative of a stronger metal–oxygen bond in the former. The shorter C(30)–O(2) and longer C(30)–O(1) bond lengths in **2** compared to **3** are also consistent with greater intraligand conjugation in the latter (Fig. 3a).

The difference in the extent of conjugation between the isoquinoline ring and the carboxylate group in **2** and **3** stems from greater steric hindrance in the 1-COO-iqu$^-$ ligand in the former than in 3-COO-iqu$^-$ in the latter. Fig. 3b shows the calculated relative energy of each free ligand, 1-COO-iqu$^-$ and 3-COO-iqu$^-$, as the dihedral angle, θ(N5–C29–C30–O1), between the carboxylate unit and the isoquinoline is systematically varied. It is evident from Fig. 3b, that for 3-COO-iqu$^-$ the lowest energy conformation is found when the carboxylate and the isoquinoline moieties are coplanar at $\theta = 0.01°$. In contrast, the minimum energy for the 1-COO-iqu$^-$ ligand is calculated at $\theta = -54.83°$, and the energy is at a maximum when the two units are coplanar. In 1-COO-iqu$^-$, a coplanar conformation results in steric clashing between one of the carboxylate oxygen atoms and the hydrogen atom in the

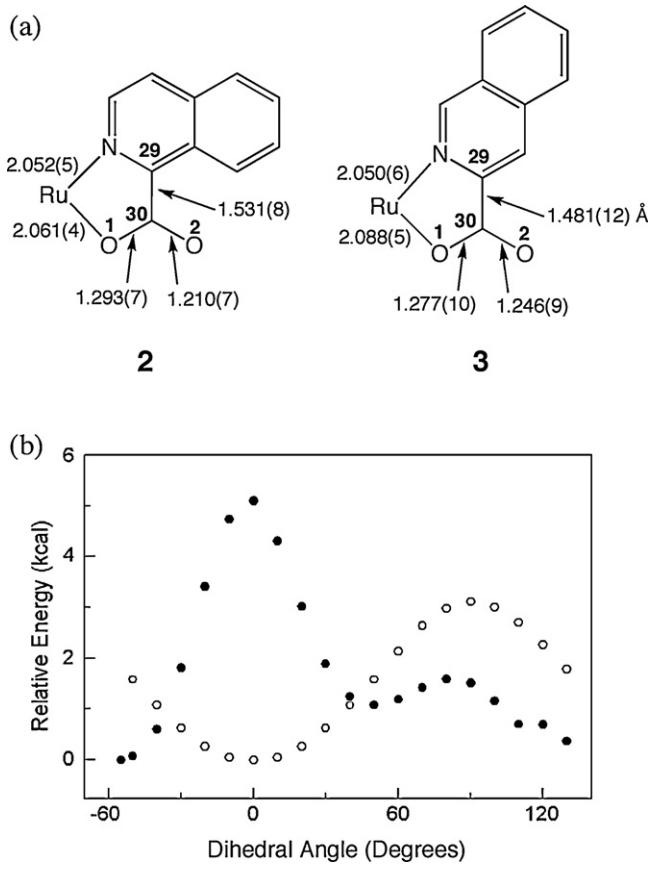

Fig. 3. Selected bond lengths (Å) in (a) **2** and **3** and (b) the relative single point energies of 1-COO-iqu$^-$ (●) and 3-COO-iqu$^-$ (○) free ligand as the carboxylate group is rotated about the isoquinoline.

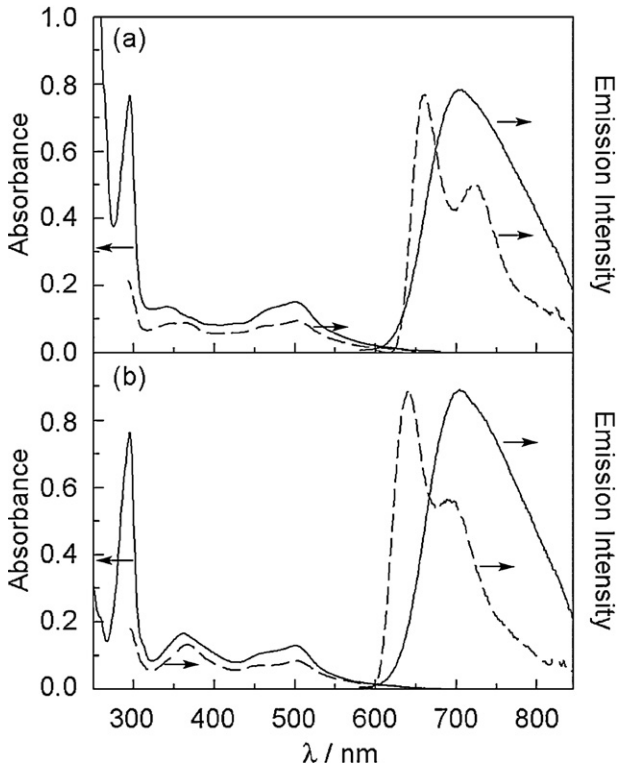

Fig. 4. Electronic absorption (—), emission (λ_{exc} = 470 nm; —), and excitation (λ_{em} = 700 nm; – – –) spectra in CH_2Cl_2 at 298 K and emission at 77 K (λ_{exc} = 470 nm; – – –) in 4:1 (v/v) EtOH/MeOH glass of (a) **2** and (b) **3**.

peri-position (H8) of the isoquinoline ring, which is alleviated by twisting of the carboxylate group out of plane with respect to the isoquinoline. This twisting that results from steric crowding by substituents located in the 1-position of naphthalene, the *peri*-effect, is well established [64–66]. There is no steric strain with hydrogen atoms of the isoquinoline ring when the carboxylate substituent is in the 3-position, as found in 3-COO-iqu$^-$, resulting in a coplanar disposition between the carboxylate and the isoquinoline. These results help explain the longer bond measured between the carboxylate and the isoquinoline carbon atoms in the 1-COO-iqu$^-$ complex **2**, and corresponding slightly shorter C(29)–C(30) bond in **3** stemming from the delocalization of the isoquinoline π-system onto the carboxylate unit in 3-COO-iqu$^-$.

3.2. Electronic absorption and emission

The electronic absorption spectra of **2** and **3** in CH_2Cl_2 are shown in Fig. 4 with maxima and extinction coefficients listed in Table 1 The transitions observed at 295 nm with ε = 24,600 M^{-1} cm^{-1} in **2** and ε = 31,400 M^{-1} cm^{-1} in **3** are assigned as bpy ππ*, similar in peak position but less intense as that in **1** (290 nm, 95,200 M^{-1} cm^{-1}) in the same solvent [67], as listed in Table 1. In addition, **2** and **3** exhibit maxima in the visible region assigned as arising from metal-to-ligand charge transfer (^{1}MLCT) transitions. The ^{1}MLCT absorption maxima are observed at 341 nm (4380 M^{-1} cm^{-1}) and 499 nm (5310 M^{-1} cm^{-1}) in **2** and similar transitions were observed at 360 nm (6790 M^{-1} cm^{-1}) and 500 nm (5260 M^{-1} cm^{-1}) in **3**. The lowest energy transitions in both **2** and **3** are assigned as Ru → bpy ^{1}MLCT and are red-shifted compared to that of **1** at 452 nm (16,000 M^{-1} cm^{-1}) in the same solvent [67]. The lower intensity of the ^{1}MLCT absorption in **2** and **3** relative to that of **1** can be explained by the presence of an additional bpy ligand in the latter [41,68]. It should be noted that the ^{1}MLCT absorption maxima of both complexes show a small solvent dependence typical of charge transfer transitions [69], shifting from 492 nm in CH_3CN to 501 nm in CH_2Br_2 in **2** and from 494 nm to 506 nm in **3** in the same solvents (Table 2).

Complexes **2** and **3** are weakly emissive at room temperature, with representative emission and excitation spectra at 298 K in CH_2Cl_2 and emission at 77 K in ethanol/methanol (4:1 v:v) glasses shown in Fig. 4. Emission maxima and quantum yields of **2** and **3** in CH_2Cl_2 are listed in Table 1. The excitation spectrum of each complex overlays well with the corresponding absorption spectrum (Fig. 4), indicating that the emission does not arise from an impurity in the sample. The 298 K emission of **2** and **3** in CH_2Cl_2, with maxima at 708 nm ($\Phi_{em} = 4.1(6) \times 10^{-4}$) and 704 nm ($\Phi_{em} = 4.8(8) \times 10^{4}$) respectively, are red-shifted and ~2 orders of magnitude weaker relative to that of **1** with maximum at 606 nm ($\Phi_{em} = 2.9 \times 10^{-2}$) in the same solvent (Table 1) [41]. The luminescence lifetimes of **2** and **3**, 124 ns and 164 ns, respectively, are shorter than that of **1** (488 ns) in CH_2Cl_2 [41]. The excited state energies (E_{00}) were estimated to be 1.89 eV and 1.95 eV from the 77 K emission spectra of **2** and **3**, in 4:1 (v/v) EtOH/MeOH, respectively (Fig. 4). The vibronic progressions observed in the 77 K emission for **2** and **3** of 1270 cm^{-1} and 1206 cm^{-1}, respectively, parallel that in **1**, 1250 cm^{-1}, under similar experimental conditions [70]. The similarity of the various emission properties of **2** and **3** to those of **1** can be used to assign the luminescence in these complexes as arising from a Ru → bpy ^{3}MLCT excited state.

The red shift in the Ru → bpy MLCT absorption and emission of **2** and **3** compared to **1** is consistent with a smaller ligand-field splitting in the former and is typical of ruthenium bis(bipyridyl) complexes with ligands in their coordination sphere that are weaker than bpy, such as *cis*-Ru(bpy)$_2$Cl$_2$ [68–71,72]. Since the

Table 1
Photophysical and electrochemical properties of complexes **1**–**3**.

Complex	λ_{abs}/nm ($\varepsilon/\times10^3$ M^{-1} cm^{-1})[a]	λ_{em}/nm (Φ_{em})[a]	$E_{1/2}$/V vs SCE[b]
1	290 (95.2), 352 (16.2)	606 (2.9×10^{-2})	+1.29[c], −1.33[c], −1.53, −1.77
2	295 (24.6), 341 (4.38), 499 (5.31)	708 (4.1×10^{-4})	+1.03[d], +0.86, −1.38, −1.57, −1.83
3	295 (31.4), 360 (6.79), 500 (5.26)	704 (4.8×10^{-4})	+1.20[d], +0.85, −1.41, −1.63, −1.99

[a] In CH_2Cl_2 at 298 K.
[b] In CH_3CN with 0.1 M $^tBu_4NPF_6$; vs SCE.
[c] Consistent with Ref. [87].
[d] Quasi-reversible.

Table 2
Solvent dependence of the absorption and emission properties of **2** and **3**.

	2			**3**		
Solvent	λ_{abs}/nm	λ_{em}/nm	Φ_{em}[a]	λ_{abs}/nm	λ_{em}/nm	Φ_{em}[a]
CH_2Cl_2	499	708	4.1	500	704	4.8
CH_2Br_2	501	710	4.2	506	713	3.9
Pyridine	497	713	1.3	500	721	2.7
CH_3CN	492	739	0.57	494	738	1.9
DMSO	496	755	0.22	494	739	2.2
THF	497	743	1.6	497	747	1.4

[a] At 298 K, $\times10^{-4}$, λ_{exc} = 470 nm.

energy of the π^* orbital of the bpy ligands is not expected to shift significantly upon variation in the coordination of the Ru(II) center [43,73,68], the observed differences are likely due to the destabilization of the metal t_{2g}-type orbitals upon substitution of a bpy ligand for 1-COO-iqu$^-$ and 3-COO-iqu$^-$ in **2** and **3**, respectively. This destabilization of the filled metal d-orbitals results in lower energy Ru → bpy ^{1}MLCT transitions explained by the presence of the oxygen atom in the coordination sphere, which is a π-donor and provides Ru–O(π^*) character to the metal-centered highest occupied molecular orbital(s) [28,68,73–76].

It is evident from Table 2 that the emission maxima and intensities of **2** and **3** are highly dependent on solvent. As the energy of the MLCT absorption and emission shifts to lower energy with solvent, the emission intensities of **2** and **3** decrease. This trend in the solvent dependence of the emission lifetimes of **2** parallel the emission intensities, with τ = 124 ns in CH_2Cl_2, 30 ns in pyridine, and 4.3 ns in DMSO. Similar results were observed for **3** with lifetimes of 164 ns in CH_2Cl_2, 93 ns in pyridine, and 59 ns in DMSO. In general, the decrease in emission intensity and lifetime with lower excited state energy can be attributed to larger non-radiative decay rate constant to the ground state. This dependence, known as the energy gap law, has been previously shown to be applicable transition metal complexes of Ru(II), Os(II), and Re(I) that possess emissive ^{3}MLCT excited states [77].

3.3. Time-resolved absorption

The transient absorption spectrum of **3** in deoxygenated DMSO is shown in Fig. 5. Immediately following the laser pulse, the transient absorption spectrum exhibits positive features from 340 nm to 400 nm and ground state bleaching from 400 nm to 600 nm. The decay kinetics measured for the signal at 370 nm and for the bleach at 500 nm are ~75 ns, which are within the detection limit of our instrument, but are qualitatively similar to the ^{3}MLCT emission lifetime of the complex in DMSO, 59 ns. Similar transient absorption spectra were recorded in other solvents for both **2** and **3** immediately after the laser pulse, which are similar to those previously reported for the transient absorption spectrum of $[Ru(bpy)_3]^{2+}$ and consistent with the ^{3}MLCT state of the complexes [78–85].

In the coordinating solvents pyridine and DMSO, long-lived transient signals were also observed for **3** with lifetimes of 49 μs and 44 μs, respectively. These long-lived transients are not observed in CH_2Cl_2 and exhibit positive absorption features at ~510 nm in both DMSO (Fig. 5) and pyridine (Fig. S1). This transient species is believed to arise from a solvent-coordinated intermediate of the type $[Ru(bpy)_2(\eta^1\text{-3-COO-iqu})(solvent)]^+$. The formation of the long-lived transient may occur by breaking of the Ru–O bond, allowing the solvent to coordinate to the metal. Although spectral features corresponding to the ^{3}MLCT state of **2** were observed immediately after the laser pulse, there was no evidence of a long-lived transient on the μs timescale for the complex in DMSO or pyridine. It is hypothesized that the stronger Ru–O bond in **2** compared to **3**, precludes the formation of the $[Ru(bpy)_2(\eta^1\text{-1-COO-iqu})(solvent)]^+$ complex in the former.

3.4. Electrochemistry and electronic structure calculations

Complexes **2** and **3** exhibit single reversible anodic waves at +0.86 V and +0.85 V vs SCE in CH_3CN (0.1 M $TBAPF_6$), respectively, that arise from the metal-centered oxidation of each complex (Table 2). These oxidation potentials show that **2** and **3** are easier to oxidize than **1** by ~0.4 V [86]. This ease in oxidation is consistent with the destabilization of the filled t_{2g}-type d-orbitals on the metal in the presence of the coordinated π-donor oxygen atom.

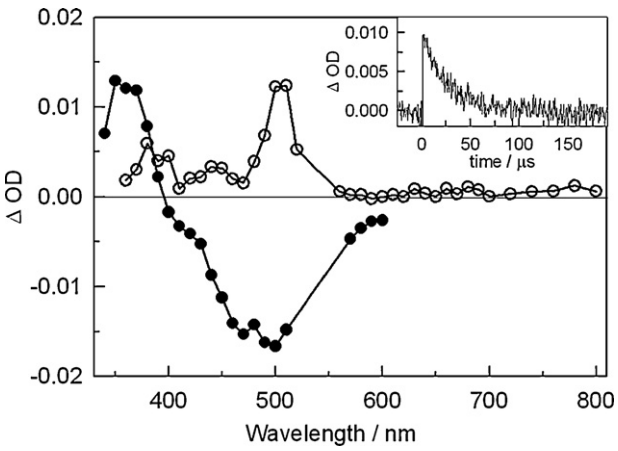

Fig. 5. Transient absorption spectra of 0.2 mM **3** in DMSO (λ_{exc} = 532 nm) immediately following the laser pulse (●) and 5 μs (○) after excitation. Inset: decay at 500 nm.

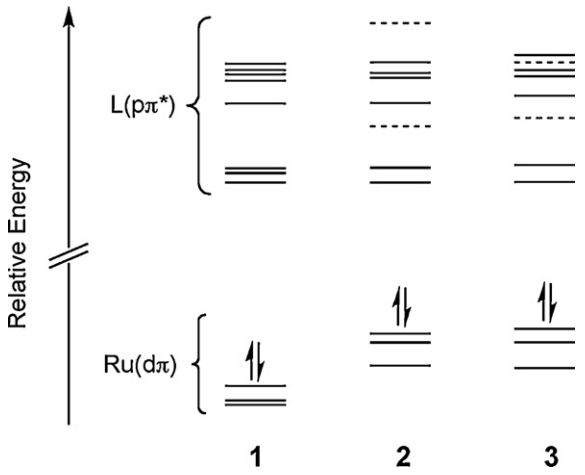

Fig. 6. MO diagrams for **1**–**3**, distinguishing the L(pπ*) orbitals with bpy(π*) contribution (—) from those with iqu(pπ*) contribution (– – –). The LUMOs were set at the same energy in all complexes.

A quasi-reversible redox couple was also observed in both **2** and **3** with E_p = +1.03 and +1.20 V vs SCE, respectively, assigned to the oxidation of the isoquinoline ligand in each complex. In addition, three well-resolved cathodic reversible waves were observed for both **2** and **3**. There is very little difference in the peak position of the first two reduction peaks in **2** and **3**, with $E_{1/2} \approx -1.4$ and −1.6 V vs SCE and correspond well with the first two reduction potentials in **1** (Table 1). Therefore, they have been assigned to the sequential reduction of each of the bpy ligands in **2** and **3**. The third reduction potential depends on the character of the isoquinoline ligand with $E_{1/2} = -1.83$ and −1.99 V vs SCE for **2** and **3**, respectively (Table 2). Using the ground state oxidation potentials for **2** and **3**, excited state oxidation potentials of −1.03 V (E_{00} = 1.89 eV) and −1.10 V (E_{00} = 1.95 eV) vs SCE can be estimated, respectively, such that these complexes are better excited state reducing agents than **1** (−0.81 V vs SCE) by 0.2–0.3 V [86].

The calculated molecular orbital (MO) diagrams for **2** and **3** predict a set of three occupied metal-centered MOs that are comprised the highest occupied molecular orbital (HOMO), HOMO-1, and HOMO-2, referred to as the Ru(dπ) set (Fig. 6). In both **2** and **3**, the lowest unoccupied molecular orbital (LUMO) and the LUMO+1 are bpy(π*) followed by the LUMO+2, which is iqu(π*) in character, consistent with the assignments made from the electrochemical data. A decrease in the HOMO–LUMO gap of 0.41 eV and 0.35 eV for **2** and **3**, respectively, as compared to **1**, is predicted when single point calculations of the optimized gas-phase molecules are performed in CH_3CN. This result is in good agreement with the experimentally determined decrease in the HOMO–LUMO gap of 0.38 V and 0.36 V for **2** and **3** from the electrochemistry data, as compared to **1** in the same solvent. The similarity in the first reduction potentials for **1**–**3** show that the energy of the LUMO bpy(π*) orbitals in all three complexes are not expected to vary among the complexes. Therefore, the LUMOs of **1**–**3** were set equal with respect to each other and the decrease in the HOMO–LUMO gap of **2** and **3** can be attributed to the destabilization of the Ru(dπ) orbitals (Fig. 6).

Time-dependent DFT (TD-DFT) calculations were performed in the gas phase to predict the transition energies. Because of the low dielectric constant of CH_2Cl_2, D_s = 6.7 [87], the TD-DFT calculations on the gas-phase optimized structure accurately model the experimental transition maxima. The calculated transitions for **2** and **3** at λ > 305 nm are listed in Table 3 with the corresponding oscillator strength (*f*). The computational results confirm the assignment of the lowest energy spin-allowed transitions for **2** and **3** as Ru(dπ) → bpy(π*) ^{1}MLCT with the lowest energy peaks with maxima at 496 nm (*f* = 0.1067) and 494 nm (*f* = 0.1082) for **2** and **3**, respectively, in good agreement with the experimental maxima listed in Table 1.

Table 3
Calculated vertical singlet excitations and oscillator strength (*f*) of **2** and **3**.[a]

λ_{abs}/nm (*f*)	
2	**3**
325(0.0307)	319(0.0206)
326(0.0639)	325(0.0252)
347(0.0538)	345(0.0336)
364(0.0566)	354(0.1101)
383(0.0282)	369(0.0304)
389(0.0539)	371(0.0225)
395(0.0216)	375(0.0367)
469(0.0481)	465(0.0368)
496(0.1067)	494(0.1082)

[a] Only transitions with *f* > 0.02 are listed; all transition assignments were made from the character of the orbitals most involved in each transition and were determined to be Ru → bpy MLCT in character.

3.5. Excited state electron transfer

Owing to the relatively low emission quantum yield and shorter lifetime of **2**, the electron transfer studies were undertaken only with **3**. The transient absorption spectra of **3** in the presence of 6 mM methyl viologen (MV^{2+}) collected after 6.5 μs and 104 μs after excitation in deoxygenated DMSO are shown in Fig. 7. After the excitation of **3** with MV^{2+} in DMSO, the transient absorption spectrum after 6.5 μs shows evidence of both the long-lived transient of the complex with maximum at 510 nm and reduced methyl viologen, $MV^{\bullet+}$, with as strong peak at ~390 nm [88]. As expected from the results in Fig. 5, the decay recorded at 510 nm (Fig. 7 inset; red) corresponds to the long-lived species with a lifetime of 38 μs, but after 104 μs the absorption features remaining correspond to $MV^{\bullet+}$ (Fig. 7). It is clear from the data in Fig. 6 that the electron transfer to generate $MV^{\bullet+}$ stems from the ^{3}MLCT excited state of the complex and that the solvent-coordinated transient species is unaffected by the presence of the acceptor in solution. Stern–Volmer plots of the emission quenching of **3** by MV^{2+} results in a quenching rate constant of 5.9×10^9 M^{-1} s^{-1}, for which $\Delta G \sim -0.67$ V, is similar to values reported by others for **1** [86,89]. It is evident from the inset of Fig. 7 (black) that the decay at 390 nm is significantly longer than that of the isomer, with a second order rate constant for the back

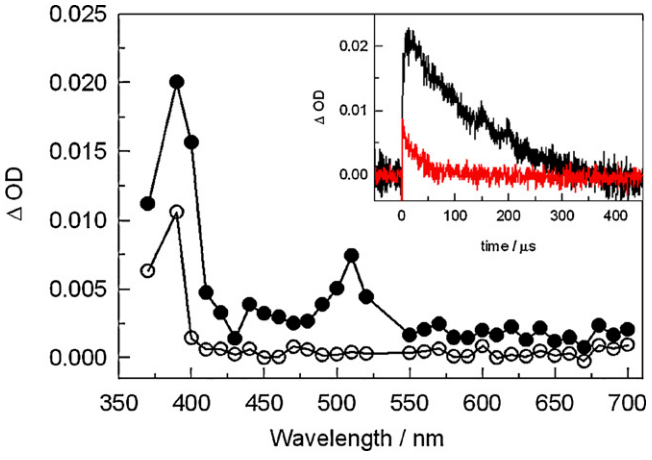

Fig. 7. Transient absorption spectra of 0.2 mM **3** in DMSO (λ_{exc} = 532 nm) in the presence of 6 mM MV^{2+} 6.5 μs (○) and 104 μs (●). Inset: decays at 390 nm (black) and 500 nm (red). (For interpretation of the references to color in this figure legend, the reader is referred to the web version of the article.)

electron transfer estimated to be $\sim 10^9\ M^{-1}\ s^{-1}$ ($\Delta G \sim -1.3$ V), similar to values reported for the bimolecular back electron transfer from $MV^{\bullet+}$ to oxidized **1** [88].

4. Conclusions

Two new ruthenium(II) complexes possessing the isoquinoline carboxylate ligands, $Ru(bpy)_2(1\text{-}COO\text{-}iqu)]^+$ (**2**) and $[Ru(bpy)_2(3\text{-}COO\text{-}iqu)]^+$ (**3**), were synthesized and characterized, and their crystal structures were determined. The 1-COO-iqu$^-$ and 3-COO-iqu$^-$ ligands coordinate to the Ru(II) center via the aromatic nitrogen and one carboxylate oxygen atom. The presence of the oxygen atom in the coordination sphere reduces the ligand-field splitting of these complexes compared to $[Ru(bpy)_3]^{2+}$ (**1**), thus shifting the MLCT absorption and emission to lower energies and making **2** and **3** easier to oxidize in the ground state and better excited state reducing agents. Complexes **2** and **3** exhibit lower emission quantum yields and shorter excited state lifetimes than **1**, with $\Phi_{em} = 4.1 \times 10^{-4}$ ($\tau = 124$ ns) and $\Phi_{em} = 4.8 \times 10^{-4}$ ($\tau = 164$ ns), respectively ($\lambda_{exc} = 470$ nm). Transient absorption spectroscopy of **3** in DMSO and pyridine revealed the ^{3}MLCT excited state a early times and a long-lived transient assigned to solvent-coordinated species that regenerates the starting material with lifetimes of 49 μs and 44 μs, respectively. It is believed that the initial excitation results in the formation of both the ^{3}MLCT and the solvent-coordinated transient, and the former can reduce methyl viologen. The solvent dependence of the decay of the ^{3}MLCT states of **2** and **3** follow the energy-gap law. Calculations on the free ligands, together with the crystal structures of the complexes and time-resolved absorption, were utilized to explain the differences in the photophysical properties. The greater excited state oxidation potentials of the ^{3}MLCT states of Ru(II) complexes with an oxygen atom in the coordination sphere may also lead to new systems for photoinduced electron injection to semiconductors with larger bandgaps.

Acknowledgements

C.T. thanks the National Science Foundation (CHE-0911354), the Ohio Supercomputer Center, and the Center for Chemical and Biochemical Dynamics for their generous support. D.A.L. thanks the OSU Graduate School for an OSU Presidential Fellowship.

Appendix A. Supplementary data

Supplementary data associated with this article can be found, in the online version, at doi:10.1016/j.jphotochem.2010.09.025.

References

[1] (a) M. Wang, N. Chamberland, L. Breau, M. Livain, J.-E. Moser, R. Humphry-Baker, B. Marsan, S.M. Zakeeruddin, M. Graetzel, Michael, Nat. Chem. 2 (2010) 385–389;
(b) M. Gratzel, Acc. Chem. Res. 42 (2009) 1788–1798;
(c) M.K. Nazeeruddin, C. Klein, P. Liska, M. Graetzel, Coord. Chem. Rev. 249 (2005) 1460;
(d) M. Gratzel, Nature 414 (2001) 338.
[2] (a) A.J. Esswein, D.G. Nocera, Chem. Rev. 107 (2007) 4022–4047;
(b) N.S. Lewis, D.G. Nocera, Proc. Natl. Acad. Sci. 103 (2006) 15729.
[3] (a) K. Kils, E.I. Mayo, B.S. Brunschwig, H.B. Gray, N.S. Lewis, J.R. Winkler, J. Phys. Chem. B 108 (2004) 15640–15651;
(b) K. Kils, E.I. Mayo, D. Kuciauskas, R. Villahermosa, N.S. Lewis, J.R. Winkler, H.B. Gray, B. Harry, J. Phys. Chem. A 107 (2003) 3379–3383;
(c) D. Kuciauskas, M.S. Freund, H.B. Gray, J.R. Winkler, N.S. Lewis, J. Phys. Chem. B 105 (2001) 392–403.
[4] (a) A.J. Morris, G.J. Meyer, E. Fujita, Acc. Chem. Res. 42 (2009) 1983–1994;
(b) M. Abrahamsson, O. Taratula, P. Persson, E. Galoppini, G.J. Meyer, J. Photochem. Photobiol., A: Chem. 206 (2009) 155–163;
(c) S. Ardo, G.J. Meyer, Chem. Soc. Rev. 38 (2009) 115–164.
[5] (a) M.H. Lim, H. Song, E.D. Olmon, E.E. Dervan, J.K. Barton, Inorg. Chem. 48 (2009) 5392–5397;
(b) B.M. Zeglis, J.A. Boland, J.K. Barton, Biochemistry 48 (2009) 839–849;
(c) C.A. Puckett, J.K. Barton, J. Am. Chem. Soc. 129 (2007) 46;
(d) M.A. O'Neill, J.K. Barton, Top. Curr. Chem. 236 (2004) 67;
(e) T.G. Drummond, M.G. Hill, J.K. Barton, Nat. Biotechnol. 21 (2003) 1192.
[6] S. Aoki, M. Zulkefeli, M. Shiro, M. Kohsako, K. Takeda, E. Kimura, J. Am. Chem. Soc. 127 (2005) 9129–9139.
[7] (a) M. Li, P. Lincoln, J. Inorg. Biochem. 103 (2009) 963–970;
(b) P. Nordell, F. Westerlund, A. Reymer, A.H. El-Sagheer, T. Brown, B. Norden, P. Lincoln, J. Am. Chem. Soc. 130 (2008) 14651;
(c) F.R. Svensson, M. Li, B. Norden, P. Lincoln, J. Phys. Chem. B 112 (2008) 10969.
[8] (a) Y. Sun, C. Turro, Inorg. Chem. 49 (2010) 5025–5032;
(b) Y. Sun, Y. Liu, C. Turro, J. Am. Chem. Soc. 132 (2010) 5594–5595;
(c) Y. Sun, S.N. Collins, L.E. Joyce, C. Turro, Inorg. Chem. 49 (2010) 4257–4262;
(d) D.A. Lutterman, A. Chouai, Y. Sun, C.D. Stewart, K.R. Dunbar, C. Turro, J. Am. Chem. Soc. 130 (2008) 1163–1170;
(e) Y. Sun, D.A. Lutterman, C. Turro, Inorg. Chem. 47 (2008) 6427;
(f) Y. Liu, A. Chouai, N.N. Degtyareva, K.R. Dunbar, C. Turro, J. Am. Chem. Soc. 127 (2005) 10796.
[9] (a) Y. Sun, Yujie; M. El Ojaimi, R. Hammitt, R.P. Thummel, C. Turro, J. Phys. Chem. B, in press;
(b) A. Chouai, S.E. Wicke, C. Turro, J. Bacsa, K.R. Dunbar, D. Wang, R.P. Thummel, Inorg. Chem. 44 (2005) 5996.
[10] K.-F. Chow, F. Mavre, R.M. Crooks, J. Am. Chem. Soc. 130 (2008) 7544–7545.
[11] K.K.-W. Lo, W.-K. Hui, C.-K. Chung, K.H.-K. Tsang, T.K.-M. Lee, C.-K. Li, J.S.-Y. Lau, D.C.-M. Ng, Coord. Chem. Rev. 250 (2006) 1724.
[12] (a) Z.N. da Rocha, M.S.P. Marchesi, J.C. Molin, C.N. Lunardi, K.M. Miranda, L.M. Bendhack, P.C. Ford, R.S. da Silva, Dalton Trans. (2008) 4282–4287;
(b) R. Santana da Silva, M.S.P. Marchesi, A.C. Tedesco, A. Mikhailovsky, P.C. Ford, Photochem. Photobiol. Sci. 6 (2007) 515–518.
[13] (a) Y. Liu, R. Hammitt, D.A. Lutterman, R.P. Thummel, C. Turro, Inorg. Chem. 46 (2007) 6011;
(b) Y. Liu, R. Hammitt, D.A. Lutterman, L.E. Joyce, R.P. Thummel, C. Turro, Inorg. Chem. 48 (2009) 375;
(c) Y. Liu, D.B. Turner, T.N. Singh, A. Chouai, K.R. Dunbar, C. Turro, J. Am. Chem. Soc. 131 (2009) 26–27;
(d) R. Zhao, R. Hammitt, R.P. Thummel, Y. Liu, C. Turro, R.M. Snapka, Dalton Trans. 48 (2009) 10926–10931;
(e) Y. Sun, L.E. Joyce, N.M. Dickson, C. Turro, Chem. Commun. 46 (2010) 2426;
(f) Y. Sun, L.E. Joyce, N.M. Dickson, C. Turro, Chem. Commun., in press.
[14] (a) M.J. Clarke, Coord. Chem. Rev. 236 (2003) 209–233;
(b) M.J. Clarke, Coord. Chem. Rev. 232 (2002) 69.
[15] (a) V. Balzani, G. Bergamini, F. Marchioni, P. Ceroni, Coord. Chem. Rev. 250 (2006) 1254;
(b) V. Balzani, A. Juris, Coord. Chem. Rev. 211 (2001) 97.
[16] (a) D. Kuciauskas, J.E. Monat, R. Villahermosa, H.B. Gray, N.S. Lewis, J.K. McCusker, J. Phys. Chem. B 106 (2002) 9347;
(b) J.E. Monat, J.H. Rodriguez, J.K. McCusker, J. Phys. Chem. A 106 (2002) 7399.
[17] A. Vlcék, Coord. Chem. Rev. 200 (2000) 933.
[18] (a) C.A. Kelly, G.J. Meyer, Coord. Chem. Rev. 211 (2001) 295;
(b) G.J. Meyer, Inorg. Chem. 44 (2005) 6852.
[19] N.D. McClenaghan, Y. Leydet, B. Maubert, M.T. Indelli, S. Campagna, Coord. Chem. Rev. 249 (2005) 1336.
[20] E.A. Medlycott, G.S. Hanan, Coord. Chem. Rev. 250 (2006) 1763.
[21] (a) B.A. McClure, E.R. Abrams, J.J. Rack, J. Jeffrey, J. Am. Chem. Soc. 132 (2010) 5428–5436;
(b) B.A. McClure, J.J. Rack, Angew. Chem., Int. Ed. 48 (2009) 8556–8558;
(c) B.A. McClure, J.J. Rack, Angew. Chem., Int. Ed. 48 (2009) 8556;
(d) D.A. Lutterman, A.A. Rachford, J.J. Rack, C. Turro, J. Phys. Chem. A 113 (2009) 11002;
(e) B.A. McClure, N.V. Mockus, D.P. Butcher, D.A. Lutterman, C. Turro, J.L. Petersen, J.J. Rack, Inorg. Chem. 48 (2009) 8084.
[22] (a) T.N. Singh, C. Turro, Inorg. Chem. 43 (2004) 7260;
(b) Y. Liu, D.B. Turner, T.N. Singh, A. Chouai, K.R. Dunbar, C. Turro, J. Am. Chem. Soc. 131 (2009) 26.
[23] (a) P.C. Ford, S. Wecksler, Coord. Chem. Rev. 249 (2005) 1382;
(b) P.C. Ford, B.O. Fernandez, M.D. Lim, Chem. Rev. 105 (2005) 2439;
(c) R.S. da Silva, M.S.P. Marchesi, C. Khin, C.N. Lunardi, L.M. Bendhack, P.C. Ford, J. Phys. Chem. B 111 (2007) 6962;
(d) P.C. Ford, L.E. Laverman, Coord. Chem. Rev. 249 (2005) 391.
[24] A.K.M. Holanda, F.O.N. da Silva, J.R. Sousa, I.C.N. Diogenes, I.M.M. Carvalho, I.S. Moreira, M.J. Clarke, L.G.F. Lopes, Inorg. Chim. Acta 361 (2008) 2929.
[25] M.J. Rose, P.K. Mascharak, Coord. Chem. Rev. 252 (2008) 2093.
[26] (a) J.-P. Collin, V. Heitz, J.-P. Sauvage, Top. Curr. Chem. 262 (2005) 29;
(b) S. Bonnet, J.-P. Collin, M. Koizumi, P. Mobian, J.-P. Sauvage, Adv. Mater. 18 (2006) 1239;
(c) S. Bonnet, J.-P. Collin, Chem. Soc. Rev. 37 (2008) 1207.
[27] (a) P.C. Ford, Coord. Chem. Rev. 5 (1970) 75;
(b) P.C. Ford, Coord. Chem. Rev. 44 (1982) 61;
(c) P.C. Ford, D. Wink, J. Dibenedetto, Prog. Inorg. Chem. 30 (1983) 213.
[28] J. Van Houten, R.J. Watts, Inorg. Chem. 17 (1978) 3381.
[29] E. Tfouni, Coord. Chem. Rev. 196 (2000) 281.
[30] V. Balzani, V. Carasitti, Photochemistry of Coordination Compounds, Academic Press, New York, 1975.
[31] D.V. Pinnick, B. Durham, Inorg. Chem. 23 (1984) 1440.

[32] B. Durham, J.V. Caspar, J.K. Nagle, T.J. Meyer, J. Am. Chem. Soc. 104 (1982) 4803.
[33] M. Gleria, F. Minto, G. Beggiato, P.J. Bortolus, Chem. Soc., Chem. Commun. (1978) 285.
[34] M. Irie, Chem. Rev. 100 (2000) 1685.
[35] H. Tian, S. Yang, Chem. Soc. Rev. 33 (2004) 85.
[36] (a) J.J. Rack, J.R. Winkler, H.B. Gray, J. Am. Chem. Soc. 123 (2001) 2432;
(b) J.J. Rack, N.V. Mockus, Inorg. Chem. 42 (2003) 5792;
(c) J.J. Rack, A.A. Rachford, A.M. Shelker, Inorg. Chem. 42 (2003) 7357;
(d) A.A. Rachford, J.L. Petersen, J.J. Rack, Inorg. Chem. 44 (2005) 8065;
(e) A.A. Rachford, J.L. Petersen, J.J. Rack, Inorg. Chem. 45 (2006) 5953;
(f) A.A. Rachford, J.J. Rack, J. Am. Chem. Soc. 128 (2006) 14318;
(g) D.P. Butcher Jr., A.A. Rachford, J.L. Petersen, J.J. Rack, Inorg. Chem. 45 (2006) 9178.
[37] B.P. Sullivan, D.J. Salmon, T.J. Meyer, Inorg. Chem. 17 (1978) 3334.
[38] P.J. Giordano, C.R. Bock, M.S. Wrighton, J. Am. Chem. Soc. 100 (1978) 6960.
[39] R.A. Palmer, T.S. Piper, Inorg. Chem. 5 (1966) 864.
[40] H.T. Uyeda, Y. Zhao, K. Wostyn, I. Asselberghs, K. Clays, A. Persoons, M.J. Therien, J. Am. Chem. Soc. 124 (2002) 13806.
[41] J.V. Caspar, T.J. Meyer, J. Am. Chem. Soc. 105 (1983) 5583.
[42] J.N. Demas, G.A. Crosby, J. Phys. Chem. 75 (1971) 991.
[43] J.T. Warren, W. Chen, D.H. Johnston, C. Turro, Inorg. Chem. 38 (1999) 6187.
[44] J.S. Buterbaugh, J.P. Toscano, W.L. Weaver, J.R. Gord, C.M. Hadad, T.L. Gustafson, M.S. Platz, J. Am. Chem. Soc. 119 (1997) 3580.
[45] Z. Otwinowski, W. Minor, Macromolecular crystallography, part A, in: C.W. Carter Jr., R.M. Sweet (Eds.), Methods in Enzymology, vol. 276, Academic Press, New York, 1997, pp. 307–326.
[46] teXsan: Crystal Structure Analysis Package, version 1.7-2., Molecular Structure Corporation, The Woodlands, TX, 1995.
[47] G.M. Sheldrick, Acta Crystallogr., A 46 (1990) 467–473.
[48] G.M. Sheldrick, SHELXL-97, Acta Crystallogr., A 64 (2008) 112–122.
[49] P. Van der Sluis, A.L. Spek, Acta Crystallogr., A 46 (1990) 194–201.
[50] A.L. Spek, Acta Crystallogr., A 46 (1990) C-34.
[51] A.J.C. Wilson, E. Prince, International Tables for Crystallography Volume C, Mathematical, Physical and Chemical Tables, Kluwer Academic Publishers, Dordrecht, 1992.
[52] M.J. Frisch, Gassian 03, Revision C.02, Gaussian, Inc., Wallingford, CT, 2004, full author list provided in the Supporting Information.
[53] A.D. Becke, Phys. Rev. A: Gen. Phys. 38 (1988) 3098.
[54] A.D. Becke, J. Chem. Phys. 98 (1993) 5648.
[55] C. Lee, W. Yang, R.G. Parr, Phys. Rev. B: Condens. Matter. Mater. Phys. 37 (1988) 785.
[56] W.J. Hehre, L. Radom, P.V.R. Schleyer, J.A. Pople, Ab Initio Molecular Orbital Theory, John Wiley & Sons, New York, 1986.
[57] M. Dolg, H. Stoll, H. Preuss, Theor. Chim. Acta 85 (1993) 441.
[58] U. Wedig, M. Dolg, H. Stoll, Quantum Chemistry: The Challenge of Transition Metals and Coordination Chemistry, 1986, Dordrecht, The Netherlands.
[59] M.T. Cances, B. Mennucci, J.J. Tomasi, Chem. Phys. 107 (1997) 3032.
[60] J. Tomasi, M. Persico, Chem. Rev. 94 (1994) 2027.
[61] P. Flükiger, H.P. Lüthi, S. Portmann, J. Weber, MOLEKEL 4.3, Swiss Center for Scientific Computing, Manno, Switzerland, 2000, www.cscs.ch/molekel.
[62] J.M. Harrowfield, A.N. Sobolev, Aust. J. Chem. 47 (1994) 763.
[63] E. Krausz, H. Riesen, A.E. Rae, Aust. J. Chem. 48 (1995) 929.
[64] V. Balasubramaniyan, Chem. Rev. 66 (1966) 567.
[65] M. Pittelkow, U. Boas, M. Jessing, K.J. Jensen, J.B. Christensen, Org. Biomol. Chem. 3 (2005) 2441.
[66] M. Pittelkow, J.B. Chrstensen, T.I. Solling, Org. Biomol. Chem. 3 (2005) 508.
[67] B. Durham, J.L. Walsh, C.L. Carter, T.J. Meyer, Inorg. Chem. 19 (1980) 860.
[68] C.W. Roger, Y. Zhang, B.O. Patrick, W.E. Jones Jr., M.O. Wolf, Inorg. Chem. 41 (2002) 1162.
[69] P. Chen, T.J. Meyer, Chem. Rev. 98 (1998) 1439.
[70] B.J. Coe, D.W. Thompson, C.T. Culbertson, J.R. Schoonover, T.J. Meyer, Inorg. Chem. 34 (1995) 3385.
[71] G. Albano, P. Belser, L. De Cola, M.T. Gandolfi, Chem. Commun. (1999) 1171.
[72] S.M. Draper, D.J. Gregg, E.R. Schofield, W.R. Browne, M. Duati, J.G. Vos, P. Passaniti, J. Am. Chem. Soc. 126 (2004) 8694.
[73] D.L. Reger, J.R. Gardinier, M.D. Smith, P.J. Pellechia, Inorg. Chem. 42 (2003) 482.
[74] L.A. Ortiz-Frade, L. Ruiz-Ramirez, I. Gonzalez, A. Marin-Becerra, M. Alcarazo, J.G. Alvarado-Rodriguez, R. Moreno-Esparza, Inorg. Chem. 42 (2003) 1825.
[75] W.F. Wacholtz, R.A. Auerbach, R.H. Schmehl, Inorg. Chem. 25 (1986) 227.
[76] W.M. Wacholtz, R.A. Auerbach, R.H. Schmel, M. Ollino, W.R. Chery, Inorg. Chem. 24 (1985) 1758.
[77] (a) J.V. Caspar, E.M. Kober, B.P. Sullivan, T.J. Meyer, J. Am. Chem. Soc. 104 (1982) 630;
(b) J.V. Caspar, T.J. Meyer, J. Phys. Chem. 87 (1983) 952;
(c) E.M. Kober, J.V. Caspar, R.S. Lumpkin, T.J. Meyer, J. Phys. Chem. 90 (1986) 3722;
(d) J.A. Treadway, B. Loeb, R. Lopez, P.A. Anderson, F.R. Keene, T.J. Meyer, Inorg. Chem. 35 (1996) 2242.
[78] N.H. Damrauer, G. Cerullo, A. Yeh, T.R. Boussie, C.V. Shank, J.K. McCusker, Science 275 (1997) 54.
[79] S. Wallin, J. Davidsson, J. Modin, L. Hammarström, J. Phys. Chem. A 109 (2005) 4697.
[80] A. Yoshimura, M. Hoffman, H.J. Sun, Photochem. Photobiol. A: Chem. 70 (1993) 29.
[81] K. Kalyanasundaram, Coord. Chem. Rev. 46 (1982) 159.
[82] A. Juris, V. Balzani, F. Barigelletti, P. Belser, A. Von Zelewsky, Coord. Chem. Rev. 84 (1988) 85.
[83] R. Malone, D.J. Kelley, Chem. Phys. 95 (1991) 8970.
[84] E. Kônig, S. Kremer, Chem. Phys. Lett. 5 (1969) 87.
[85] M. Hoffman, M. Simic, Q. Mulazzani, S. Emmi, P. Fuochi, M. Venturi, Radiat. Phys. Chem. 12 (1978) 111.
[86] C.R. Bock, J.A. Connor, A.R. Gutierrez, T.J. Meyer, D.G. Whitten, B.P. Sullivan, J.K. Nagle, J. Am. Chem. Soc. 101 (1979) 4815.
[87] A.J. Gordon, R.A. Ford, The Chemist's Companion: A Handbook of Practical Data, Techniques, and References, John Wiley & Sons, New York, 1972.
[88] M.A.J. Rodgers, J.C. Becker, J. Phys. Chem. 80 (1980) 2084.
[89] C.R. Bock, T.J. Meyer, D.G. Whitten, J. Am. Chem. Soc. 96 (1974) 4710.